PREDICTION OF THE BUCKLING OF THERMOPLASTIC PRODUCTS

J. L. Spoormaker, I. D. Skrypnyk*, A. J. Heidweiller

Faculty of Design, Engineering and Production, Delft University of Technology, Netherlands
*Goodyear Research Laboratories, Akron, USA

Abstract: *Plastic bottle crates are required to weight as little as possible for lower material consumption and for transportation costs. The reliability and sustainability of crates is required to be very high. It is possible to satisfy the weight requirements by applying structural optimisation. Buckling is an imported restrain because of the decrease in load carrying capacity. Presented is the development of methods to predict the buckling behaviour of structural elements accounting for the non-linear time dependent behaviour of High Density Polyethylene. The procedure for characterising the non-linear visco-elastic behaviour of polymers is shortly described. The subroutine to account for the non-linear visco-elastic behaviour in finite element methods is outlined. A few examples of the achievements with structural elements are given.*

INTRODUCTION

We aim at predicting the buckling of a HDPE crate for beer bottles as depicted in Figure 1. Bottle crates, with (filled) bottles, are required to be stored on pallets, from several days to even weeks. The pallets are stacked one on top the other, resulting in a very high load on the bottom crate.
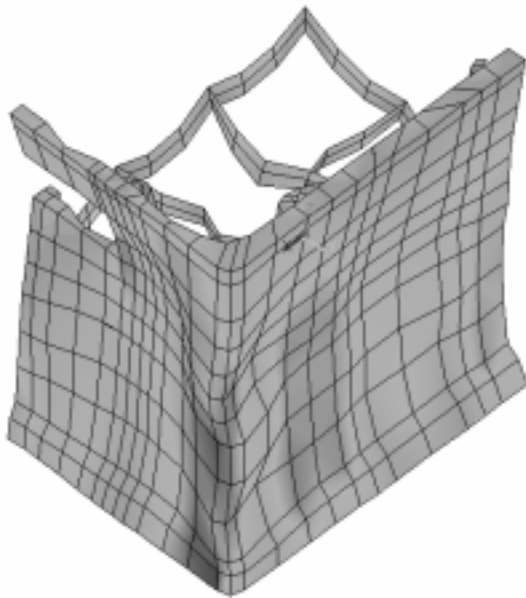
Figure 1. *One quarter of a buckled bottle crate.*

Buckling of the corner stiffening ribs of crates will cause the drop of pallets resulting in a loss the beer bottles and crates, but moreover this might injure people. A serious problem is that buckling can happen after an extended period of time. Obviously, the buckling of a crate's corner occurs after the material creeps under compressive loading.

Predicting the long term buckling behaviour in the design stage yields a possibility to optimise the design and to avoid costly mould changes and delay in delivery of crates.

The objective of the research is to predict using Finite Element Method (FEM), the onset of buckling of plastic bottle crates under compressive loading.

The creep behaviour of HDPE has been determined using tensile specimens. The nonlinear visco-elastic behaviour is characterized using non linear parameter estimation procedures.

During the first stage of the investigation, the buckling behaviour of simple HDPE test specimens (strips and U-profiles) has been studied, experimentally as well as numerically, in order to obtain better understanding of creep induced buckling. The experiments and simulations with visco-elastic strips allowed us to study creep induced buckling in comparison to traditional Euler's buckling of elastic materials. The U-profile specimens have been chosen, to investigate buckling behaviour of simple elements with stiffening ribs.

2. MATERIAL MODEL

2.1. The generalised Shapery Model

The non-linear visco-elasticity model [6, 7] is a generalisation of the Schapery model [8]:

$$\varepsilon\big[\sigma(t),t\big] = J_0\big[\sigma(t)\big] + \\ \sum_i^n \phi_i\big[\sigma(t)\big]\int_0^t F_i(\zeta-\zeta')\frac{\partial\, g_i\big[\sigma(\xi)\big]}{\partial\,\xi}d\xi \qquad (1)$$

The following forms for functions in equation (1) seem to be appropriate [9] for description of experimental data for many plastics:

$$J_0[\sigma] = A \cdot [\sigma + \sigma^\beta]$$

$$\varphi_i[\sigma] = \exp \gamma_i \cdot \sigma$$

$$g_i[\sigma] = D_i \cdot \sigma^{\alpha_i}$$

$$F_i(t) = 1 - \exp(-\lambda_i \cdot t). \qquad (2)$$

The parameters in these functions should be estimated, based on data from creep and recovery tests. For this the equation (1) can be rewritten as follows:

for creep

$$\hat{\varepsilon}[\sigma_k, t] = J_0[\sigma_k] + \sum_i \phi_k \cdot \sigma_k \cdot F_i(t) g_i(\sigma_k) \quad (3)$$

for recovery

$$\hat{\varepsilon}[\sigma_k, t] = \sum_i \left[F_i(\tilde{t} + t_1) - F_i(\tilde{t}) \right] g_i(\sigma_k) \sigma_k \quad (4)$$

$$\tilde{t} = t - t_1$$

There are strong advantages in choosing the time functions $F_i(t)$ in the form of Prony series. Firstly, this choice enables an efficient numerical scheme (Henriksen 1984) for calculation of convolution integrals. Secondly, it gives better possibilities for establishing the parameter identification procedure. This procedure is based on the idea of minimisation of the relative deviation between experimental data and model prediction. The resulting set of material parameters for HDPE is given in Table 1.

i	A=7.852·10⁻⁴				$\beta = 0.0$	
i	$D_{i,1}$	$\alpha_{i,1}$	$D_{i,2}$	$\alpha_{i,2}$	γ_i	λ_i
1	.1278·10⁻⁴	2.759	.259·10⁻³	1.059	-.2404·10⁻¹	10⁻¹
2	.3364·10⁻³	1.075	.591·10⁻⁵	2.872	-.1473·10⁻³	10⁻²
3	.3729·10⁻³	1.118	.967·10⁻⁵	2.740	.6727·10⁻¹	10⁻³
4	.5814·10⁻⁴	2.193	.284·10⁻⁹	6.254	.4689·10⁻¹	10⁻⁴
5	.6187·10⁻³	1.547	.675·10⁻¹¹	9.779	.9244·10⁻³	10⁻⁵
6	.4855·10⁻¹	1.637	.279·10⁻²	2.786	-3.377	10⁻⁶

Table 1. *The set of model parameters for description of HDPE*

The prediction of creep and recovery behaviour of HDPE (based on the equations (1), (2) and parameter set from the Table 1) is presented in Figures 2 & 3.
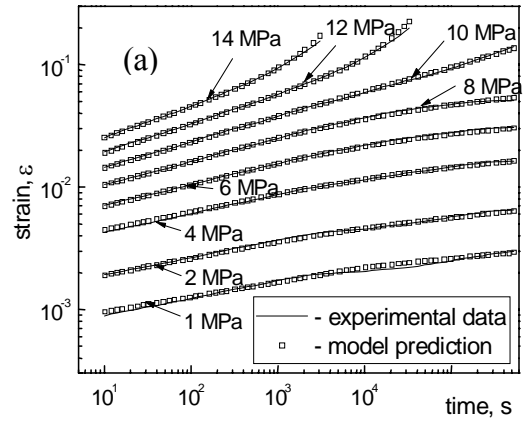
Figure 2. *Experimental data [11] and model prediction for creep of HDPE*
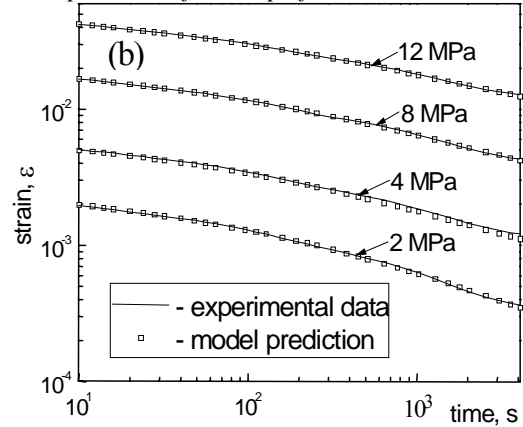
Figure 3. *Experimental data [11] and model prediction for recovery of HDPE*

2.2. Extension to 3-D formulation and Matrix formulation.

Equation (1) was extended to 3-D formulation, based on the assumptions that:
- the polymer is compressible and initially isotropic;
- the processes of change of volume and shape are uncoupled;
- the rate of viscous flow is proportional to the effective stress $\hat{\sigma}$;

As a result, equation (1) can be rewritten as follows:

$$\bar{\varepsilon} = [(1+\nu_0) \cdot M_D + (1-2\nu_0) \cdot M_H] \cdot \tilde{\varphi} \cdot (\hat{\sigma}) \cdot \bar{\sigma} +$$
$$[(1+\nu_1) \cdot M_D + (1-2\nu_1) \cdot M_H] \times$$
$$\sum_{i=1}^{n} \phi_i(\hat{\sigma}) \cdot \int_0^t F_i(t-\xi) \frac{\partial[\tilde{g}_i(\hat{\sigma})\bar{\sigma}]}{\partial \xi} \cdot d\xi$$

$$(5)$$

where

$$J_0[\sigma] = \tilde{\varphi}(\sigma) \cdot \sigma; \qquad g_i[\sigma] = \tilde{g}_i(\sigma) \cdot \sigma . \qquad (6)$$

The matrix and vector notations are:

$$\mathbf{M}_D = \begin{cases} \dfrac{2}{3}, & \text{if } i = j \text{ and } i, j \leq 3; \\[2mm] -\dfrac{1}{3}, & \text{if } i \neq j \text{ and } i, j \leq 3; \\[2mm] 2, & \text{if } i = j \text{ and } i, j > 3; \\[2mm] 0, & \text{if } i \neq j \text{ and } i, j > 3. \end{cases}$$

$$\mathbf{M}_H^{\,i,j}\Big|_{i,j=1\ldots 3} = \frac{1}{3} \qquad (7)$$

$$\bar{\sigma} = \left\{ \sigma_{xx} \; \sigma_{yy} \; \sigma_{zz} \; \tau_{xy} \; \tau_{yz} \; \tau_{zx} \right\}^T;$$

$$\bar{\varepsilon} = \left\{ \varepsilon_{xx} \; \varepsilon_{yy} \; \varepsilon_{zz} \; \gamma_{xy} \; \gamma_{yz} \; \gamma_{zx} \right\}^T. \qquad (8)$$

3. IMPLEMENTATION IN FEM-CODES

Since most of the FE packages based on the displacement formulation, the visco-elasticity model (1) of Kelvin-Voight type should be inverted and rewritten in the incremental form as follows:

$$\Delta\bar{\sigma} = \mathbf{L}\left(\Delta\bar{\varepsilon}, \Delta t \ldots\right) \qquad (9)$$

in order to be implemented into a FEA package.

Further the main elements, necessary to derive equation (9), are given. For enough regular functions $g_i(\sigma)$ (such that $\left(\partial^2\left[g_i(\sigma)\right]/\partial t^2\right) \ll 1$) the convolution integral with the exponential kernel function can be transformed to finite form, following Henriksen scheme (Henriksen 1984):

$$\int_0^t \left(1 - \exp\left(-\lambda_i(t-\xi)\right)\right)d\xi = g_i(\sigma) + \theta_i(t) \qquad (10)$$

The hereditary integral functions $\theta_i(t)$, which can be also considered as the set of internal parameters of this model:

$$\theta_i(t) = -\int_0^t \exp\left(-\lambda_i(t-\xi)\right)\frac{\partial\left[g_i(\sigma)\right]}{\partial\xi}d\xi \qquad (11)$$

can be calculated recurrently as follows:

$$\theta_i(t) = \exp\left(-\lambda_i\Delta t\right)\theta_i(t-\Delta t) - \Delta\left[g_i(\sigma)\right]\Gamma_i(\Delta t) \qquad (12)$$

Here, the following notation has been introduced for convenience:

$$\Gamma_i(\Delta t) = \frac{1 - \exp\left(-\lambda_i\Delta t\right)}{\lambda_i\Delta t} \qquad (13)$$

Further, the total differential of the equation (5) has to be derived and inverted to the form (9).

Unfortunately, numerical scheme, based on the total differential, shows low convergence ability and often becomes unstable [12]. Therefore, similar to [13], it has been assumed that the pre-integral functions $\phi_i(\sigma)$ do not vary within a time increment. In addition only partial factorisation has been used for inversion of incremental stress-strain relation (i.e. the scheme is neither completely explicit nor implicit, but a mixed one). As a result, following incremental relation has been derived [12]:

$$\Delta\bar{\sigma} = \left\{\left[\left(1+\nu_0\right)\mathbf{M}_D + \left(1-2\nu_0\right)\mathbf{M}_H\right]\tilde{\varphi}(\hat{\sigma})\right\}^{-1} \times$$
$$\{\Delta\bar{\varepsilon} - [(1+\nu_1)\mathbf{M}_D + \left(1-2\nu_1\right)\mathbf{M}_H]\times$$
$$\sum_{i=1}^n [\phi_i(\hat{\sigma})\tilde{g}_i(\hat{\sigma})(1-\Gamma_i(\Delta t))]\Delta\bar{\sigma}(t-\Delta t) +$$
$$\phi_i(\hat{\sigma})(\exp(-\lambda_i\Delta t)-1)\tilde{\theta}_i((t-\Delta t)]\} \qquad (14)$$

While deriving this relation it is implied that the loading history always starts from zero.

The above-derived scheme is recurrent. To calculate the stress increment, only data for the stresses field σ and internal parameters $\tilde{\theta}_i$ from the previous step are required. For instance, the internal parameters $\tilde{\theta}_i$ are calculated as follows:

$$\tilde{\theta}_i(t) = \exp\left(-\lambda_i\Delta t\right)\tilde{\theta}_i(t-\Delta t) - \Delta\left[\tilde{g}_i(\hat{\sigma})\bar{\sigma}\right]\Gamma_i(\Delta t) \qquad (15)$$

4. EXPERIMENTAL AND COMPUTATIONAL ASPECTS

4.1. Experiments on determining the buckling of HDPE structural elements.

Three different sets of experiments have been performed.

1. Experiments with ramp compression of strips with three different rates (5, 0.5 and 0.1 % per minute) were carried out. The maximum strain reached in these tests was 10 %.

2. Experiments were carried out with constant compressive loading. After a certain loading level (which was slightly lower, than the one necessary for instant onset of buckling) had been reached, the specimen was kept under these loading until creep buckling occurs. The time to the onset of buckling was determined.

3. Tests of ramp compression of U-profiles have been performed with a strain rate of 5% per minute until 10 % of deformation was reached.

Strips have been cut out of extruded HDPE plates and finished by milling to assure high precision and surface quality of the specimens. The cross-section of all specimens was 14.95 x 3.1 mm. The distance between clamps of the testing device will be referenced further on as to the length of the specimens. Strips with four different lengths (35, 45,

70, and 80 mm) have been tested. For the strips shorter, than 35 mm, even a small clamp misalignment drastically affects the test results. The specimens longer, than 80 mm, buckled at very low loads. This made the tests with longer strips useless because of the accuracy of the testing equipment. All tests were performed on a 10 kN Zwick testing machine with facilities for force or displacement control. The strips were clamped in the testing device. Afterwards the clamps were moved automatically to approach the zero stress level in the specimens before the test started.

As mentioned before, even a slight misalignment of the clamps can drastically influence the results of buckling tests. For instance, a small shifting (0.7 mm) of one clamp to one side, while testing a 80 mm long strip, subjected to compressive loading with a constant strain rate of 5 % per minute, leads to a drop of the buckling force by 30 % and a deviation in the post-buckling behaviour by 70 to 80 %. Therefore, special attention was paid to assure the alignment of the clamps in the testing device. As a result a good reproducibility of the experimental results was reached: for the tests with similar loading conditions and specimen length, but in different tests series, the deviation in the buckling force was less than 5 %.

The U-profiles were also manufactured from extruded HDPE plates. The wings (flanges) were bent using an electric wire bench (the bending lines were heated until bending became possible). Because of bending, some residual stresses could appear in the specimens. To avoid this, the specimens were put into a special wooden mould and heated in an oven at 90°C for half an hour. The specimens were all produced with the same width of the back wall (88mm) and of the wings (36.5 mm). The thickness of the U-profile walls was 3.1 mm. Four different lengths of specimens were chosen for tests: 256 mm, 213 mm, 170 mm and 130 mm. Again the distance between the clamps is considered as the length of the U-profiles.

Special steel clamps were produced to ensure proper clamping of the U-profile edges during testing. To verify the reproducibility of tests, at least two different specimens of the same length were used. In theory the wings of a U-profile with a perfect shape can buckle in two directions: inside and outside. In reality, the buckling mode is predefined by initial imperfections of the shape of the specimen. In the experiments both: outside and inside buckling of the wings occurred (fig. 7). For the same buckling mode the reproducibility of the experimental results was sufficient.

4.2. FEM simulation of experimental results obtained with plastic strips.

The mesh used for the FE modelling of the tests on strips consisted of quadrilateral shell elements of type 75 [14]. To simulate the clamping of the strip in the testing device, all degrees of freedom were restricted for the nodes at the top and the bottom of the specimens.

The deformation history was modelled by a step-wise function (100 loading steps). At each step the nodes at the top of the mesh were displaced at a distance, which caused -0.1% of additional deformation in the strip. To simulate the change of loading with time, the specimen was allowed to relax (**AUTO CREEP** option [15]) during the time increment, which relates to the strain rate, prescribed for the test simulated. The buckling of the loaded strips was simulated using the MARC facilities for buckling analysis (inverse power sweep method) [16]. In case, when the buckling problem involves material non-linearity (e.g. visco-elasticity in our case), the problem must be solved using a perturbation analysis.

This means, that at a certain moment of the loading history (at a certain increment), a linear buckling analysis is performed to estimate the eigenvector ϕ of the node displacements for the requested buckling mode.

At the next load increment, the node coordinates are modified to account for the fraction of the eigenvector:

$$X = X + \mathbf{f}*\phi/|\phi| \qquad (16)$$

The introduced perturbation $\{\mathbf{f}*\phi/|\phi|\}$ will grow (or diminish) in time, if the current buckling mode is stable (or unstable) under certain loading conditions. The factor $\mathbf{f}$ was found empirically. For the described model it was found to be equal to 0.5. The perturbation analysis for the first buckling mode was performed by invoking the **BUCKLE INCREMENT** option [10] right after first "deformation step" (fig. 4a).

In order to verify the accuracy of FE modelling, additional calculations with different number of elements in mesh (fig. 4a) and different number of layers in shell element (fig. 4b) were performed for the 70 mm long strip loaded by strain rate 5% per minute.
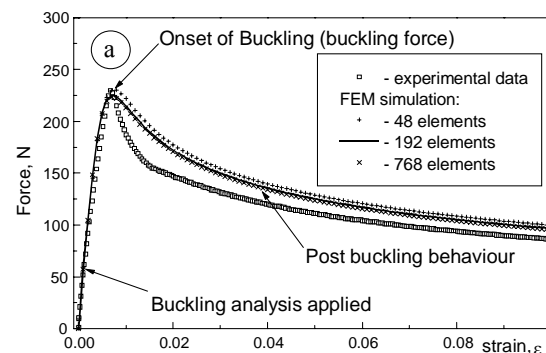
Figure 4a. *Simulation of the buckling behaviour of a 70 mm long strip for different numbers of elements.*
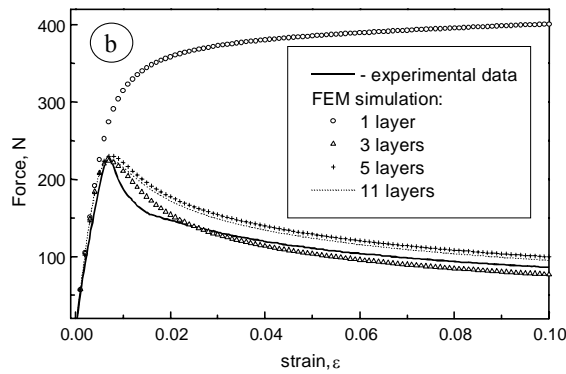
Figure 4b. *Simulation of the buckling behaviour of 70 mm long strip using different numbers of layers in the shell elements.*

For most cases (except of variant with one layer, which obviously is not functional) the accuracy of prediction of buckling force is less than 1%, while deviation between experimental data and results of simulation for post-buckling behaviour is less than 10%. Therefore, for further modelling the mesh with 48 shell elements (5 layer) was chosen.

4.3. Results of computer simulations.

The results of FE simulations of ramp compression tests with the strain rate of 5% per minute are given in figure 6. The maximum deviation between experimental data and computer prediction is less than 10% for all the strip lengths modelled.

Figure 5. FE prediction of buckling behaviour of HDPE strips with different length.
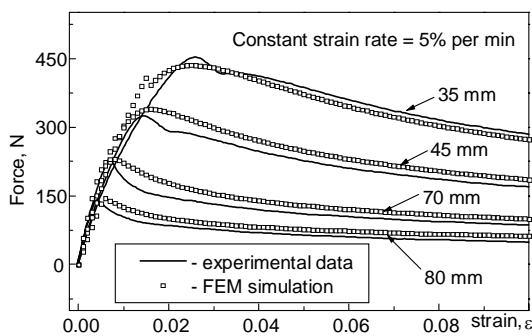
Fig. 5. *FE prediction of buckling behaviour of HDPE strips with different length.*

4.4. FEM modelling of U-profile in compression.

One quarter of the U-profile was modelled in order to save calculation time. The quadrilateral, three-dimensional shell elements of type 75 [13] with 5 layers were chosen to model the U-profile. The mesh contained 72 elements and 91 nodes. It was observed in the experiments, that a small initial sag (less than 1 mm) of the back wall of the U-profile predefines a certain buckling mode: outside or inside.
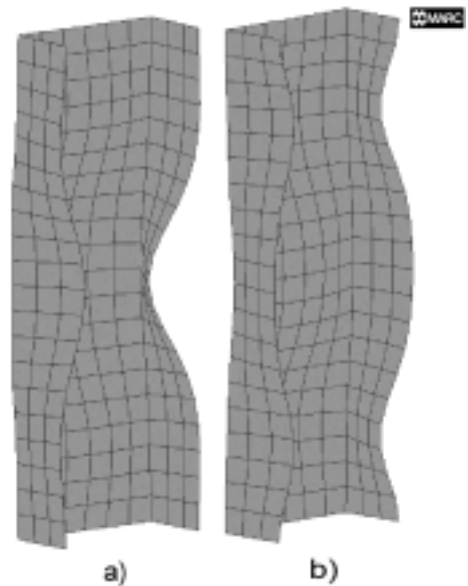
Figure 6. *Two possible modes of local buckling. (a) – wings inside, (b) - wings outside.*

This observation was confirmed by FE simulation (fig. 6). In both cases good agreement (less than 6%) between the computer prediction and the test results of compressive force was obtained (fig. 7).
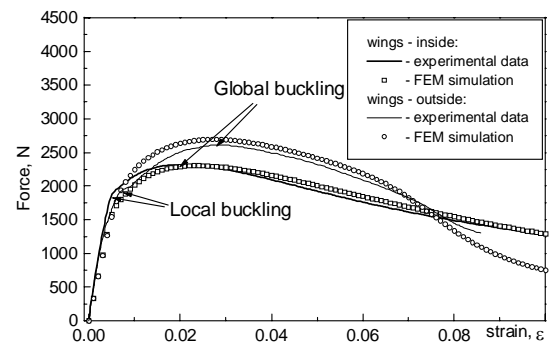
Figure 7. *Comparison of experimental and FEM simulation of U-profiles for two buckling modes.*

Because of the presence of stiffening ribs in the U-profile, buckling occurs in two steps (figures 8 & 9). First, the wings buckle that correspond to the local buckling point on fig. 4a. This leads to further buckling of the stiffening ribs.
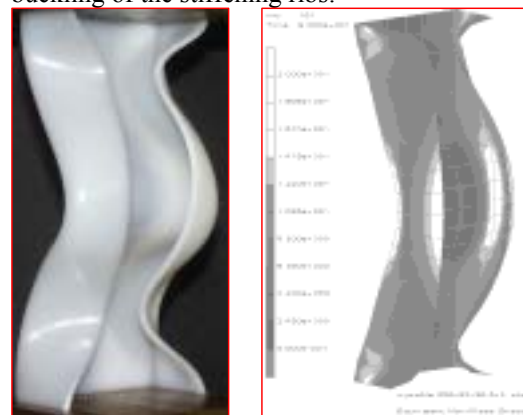
Figure 8. *Experiment and FEM simulation of inside buckling.*
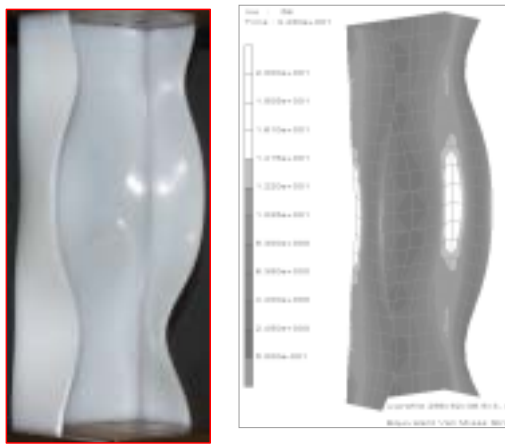
Figure 9. *Experiment and FEM simulation of outside buckling*

5. CONCLUSIONS

1. The non-linear visco-elasticity model, based on tensile creep-recovery tests, can be applied for the FEM simulation of the other types of loading of HDPE structural elements.

2. A calculation schema for FEM modelling of buckling and post-buckling behaviour of the non-linear visco-elastic strips has been established.

3. The influence of model parameters (number of elements in mesh and layers in shell element) on the accuracy of FEM calculations was determined.

4. It is shown, that established calculation model enables the prediction of the buckling and post-buckling behaviour of U-profiles under ramp compression loading.

5. The developed models can be used in the design stage and enable to design crates with reduced probability of buckling of crates in service.

References

[1] *Samuelson L.A.* Creep Deformation and Buckling of a Column with Arbitrary Cross Section. – Report No. 10, The Aeronautical Research Institute of Sweden (FFA). – 1967.

[2] *Cohen A., Arends C.B.* Creep Induced Buckling of Plastic Materials // Polym. Eng. Sci. – 1988. – **28**, No. 8, – p. 506

[3] *Cohen A., Arends C.B.* Application of a Concept of Distributed Damage to Creep Induced Buckling of High Density Polyethylene Specimens // Polym. Eng. Sci. – 1988. – **28**, No. 16, – p. 1066.

[4] *Rzanitsyn A.R.* Dokl. Akad. Nauk. SSSR, – 1946. – **52**, № 1.

[5] *Drozdov A.D., Kolmanovskii V.B.* Stability in Viscoelasticity. – Elsevier, – 1994. – 600 p.

[6] *Skrypnyk, I.D., Spoormaker, J.L.* Modelling of non-linear visco-elastic behaviour of plastic materials // Proceedings of the 5th European Conference on Advanced Materials /Euromat 97/, Materials, Functionality and Design. – 1997. – **4.** – pp. 4/491-4/495.

[7] *Skrypnyk, I.D., Zweers, E.W.G.* Non-linear visco-elastic models for polymers materials. – Technical Report K345, Faculty of Industrial Design Engineering, TU Delft, the Netherlands, – 1996. – 40 p.

[8] *Schapery, R. A.* On the Characterisation of nonlinear viscoelastic materials // J. of Polym. Eng. Sci. – 1969. – **9.** – p. 295.

[9] *Skrypnyk, I.D., Spoormaker, J.L., Kandachar, P.V.* Modelling of the long-term visco-elastic behaviour of polymeric materials. – Technical Report K369, Faculty of Industrial Design Engineering, TU Delft, the Netherlands. – 1997. – 48 p.

[10] Henriksen, M 1984. *Computers & Structures*. **18:** p.133.

[11] *Beijer J.G.J., Spoormaker J.L.* Viscoelastic behaviour of HDPE under tensile loading // Proc. of 10th International Conference on Deformation, Yield and Fracture of Polymers. – 1997. – pp.270 – 273.

[12] *Skrypnyk, I.D., Spoormaker, J.L., Vasyljkevych, T.O.* Modelling of the temperature dependent visco-elasticity in plastics. – Technical Report K381, Faculty of Design, Engineering and Production, TU Delft, the Netherlands. – 1998. – 40 p.

[13] *Lai, J.* Non-linear time-dependent deformation behaviour of high density polyethylene. – Ph.D. thesis, TU Delft, the Netherlands. – 1995. – 157 p.

[14] MARC, Element Library, Volume B, Rev. K.7, MARC Analysis Research Corp. – 1997.

[15] MARC, Program Input, Volume C, Rev. K.7, MARC Analysis Research Corp. – 1997.

[16] MARC, Theory and User Information, Volume A, Rev. K.7, MARC Analysis Research Corp. – 1997.

[17] *Oliver, P.J.* Applications of Lie groups to differential equations. – New York: Springer-Verlag New York Inc., – 1986.